Detection of Reperfusion Injury Using PET in a Monkey Model of Cerebral Ischemia

Hiroyuki Takamatsu, Hideo Tsukada, Takeharu Kakiuchi, Shingo Nishiyama, Akihiro Noda, and Kazuo Umemura

Department of Pharmacology, Hamamatsu University School of Medicine, Hamamatsu; Central Research Laboratory, Hamamatsu Photonics K.K., Shizuoka; and The Medical and Pharmacological Research Center Foundation, Ishikawa, Japan

Several studies of focal ischemia and reperfusion in animal models have proposed that reperfusion contributes to brain damage. However, the extent to which reperfusion affects the brain, especially in acute stroke patients, remains unclear. Our purpose in this study was to determine whether reperfusion injury can be detected with PET and to clarify the extent to which reperfusion contributes to brain damage. **Methods:** The right middle cerebral artery (MCA) of cynomolgus monkeys was occluded for 3 h (n = 8) or permanently (n = 5) by a transorbital device. Four consecutive PET studies were performed to assess cerebral blood flow (CBF), oxygen extraction fraction (OEF), and the cerebral metabolic rate of oxygen ($CMRO_2$). **Results:** The extent of necrotic brain damage 8 h after MCA occlusion was significantly ($P < 0.05$) greater in the transient model than in the permanent model. Cortical damage was greater in the transient model. The MCA occlusion decreased CBF and $CMRO_2$ in deep MCA territory and increased OEF in the cortex. In the permanent model, these changes continued throughout the experiment. In the transient model, the reperfusion induced postischemic hyperperfusion in the cortex, which showed necrotic damage at the end of the experiment. In this area, OEF and $CMRO_2$ were decreased by reperfusion. **Conclusion:** The results suggest that reperfusion may strongly contribute to cortical damage. PET studies revealed that reperfusion decreased OEF and $CMRO_2$ in the hyperperfused cortex. These changes may indicate reperfusion injury.

Key Words: transient cerebral ischemia; middle cerebral artery occlusion; primates; emission CT; experimental stroke

J Nucl Med 2000; 41:1409–1416

Several studies of focal ischemia and reperfusion in animal models have proposed that reperfusion contributes to brain damage (*1–3*). Abrupt reoxygenation during reperfusion is generally believed to lead to the enzymatic production of reactive oxidants (*1,2*). Therefore, several studies have involved oxygen free radicals in ischemia–reperfusion models (*4–8*).

Recent pilot clinical studies of ischemic stroke suggest that intravenous therapy with recombinant tissue plasminogen activator (t-PA) is beneficial when begun within 3 h of the onset of stroke (*9*). However, the extent to which reperfusion affects the brain, especially in patients with acute stroke, remains unclear. For optimal cerebral salvageability, a better understanding of the contribution of reperfusion injury and its mitigation is needed.

PET is a useful method of measuring oxygen metabolism. In several studies of permanent occlusion of the middle cerebral artery (MCA) in nonhuman primates, acute hemodynamic changes have been well documented with PET (*10–12*). Our purpose in this study was to determine whether reperfusion injury can be detected with PET and to clarify the extent to which reperfusion contributes to brain damage.

MATERIALS AND METHODS

Using both transient and permanent MCA occlusion models, we compared the local cerebral blood flow (CBF), oxygen extraction fraction (OEF), and cerebral metabolic rate of oxygen ($CMRO_2$) at several stages of ischemia. At the end of the experiments, the brain damage associated with both models was examined and compared. We chose cynomolgus monkeys as an experimental model of cerebral ischemia to mimic stroke in humans. In the ischemia–reperfusion model, a 3-h-long temporary occlusion of the MCA and reperfusion were used to mimic t-PA therapy in humans, because the efficacy of t-PA treatment in patients was observed within 3 h (*9*).

Animal Preparation

The studies were performed on 13 male cynomolgus monkeys (*Macaca fascicularis*) with body weights ranging from 4.7 to 6.2 kg (Clea Japan Inc., Tokyo, Japan). Eight monkeys were subjected to transient MCA occlusion, and 5 monkeys were subjected to permanent MCA occlusion. All experiments were performed in accordance with the institutional guidelines of the University of Hamamatsu School of Medicine, Hamamatsu, Japan, and the Central Research Laboratory of Hamamatsu Photonics K.K., Shizuoka, Japan.

Anesthesia was induced with 10 mg/kg intramuscular ketamine hydrochloride. The monkeys were tracheostomized, immobilized with 0.05 mg/kg intramuscular pancuronium bromide every 2 h, and artificially ventilated. Anesthesia was continued with 0.8% isoflurane in a 1:1:1 mixture of N_2O:O_2:N_2 gas during the entire experiment. The left femoral artery was catheterized for the measurement of mean arterial blood pressure and heart rate and for arterial blood sampling. The mean arterial blood pressure, heart rate, rectal temperature, arterial partial pressure of oxygen, arterial

Received Sep. 8, 1999; revision accepted Dec. 29, 1999.

For correspondence or reprints contact: Hiroyuki Takamatsu, PhD, The Medical and Pharmacological Research Center Foundation, Wo32, Inoyama-Town, Hakui-City, Ishikawa, 925-0613, Japan.

TABLE 1
Physiologic Parameters in Model of Transient Occlusion of Middle Cerebral Artery

Parameter	Before ischemia	Time after ischemia		
		2 h	4 h	6 h
MABP (mm Hg)	95 ± 18	105 ± 13	97 ± 17	97 ± 8
HR (bpm)	154 ± 23	166 ± 16	168 ± 13	169 ± 8
RT (°C)	36.9 ± 0.4	36.8 ± 0.5	37.2 ± 0.7	37.1 ± 0.5
pH	7.501 ± 0.033	7.491 ± 0.031	7.490 ± 0.029	7.485 ± 0.024
pCO_2 (mm Hg)	33.6 ± 2.4	33.1 ± 3.2	31.9 ± 3.6	32.5 ± 3.0
pO_2 (mm Hg)	195.4 ± 25.7	186.8 ± 12.3	189.1 ± 18.7	191.6 ± 13.0
Glucose (g/L)	76.7 ± 3.8	75.5 ± 8.2	80.0 ± 12.5	87.4 ± 15.4

MABP = mean arterial blood pressure; HR = heart rate; RT = rectal temperature; pCO_2 = partial pressure of carbon dioxide; pO_2 = partial pressure of oxygen.
Data are mean ± SD.

partial pressure of carbon dioxide, pH, and plasma glucose levels were continuously or regularly monitored. The right MCA was occluded by a transorbital approach (*13*). After the administration of 0.05 mg/kg intramuscular atropine, the right globe was removed. The head of the monkey was then fixed in a plastic stereotactic apparatus (SFCT-RB-PR-2; Hamamatsu Photonics K.K.) that had already been fixed in the PET scanner gantry (SHR7700; Hamamatsu Photonics K.K.) by means of a laser beam system so that head positioning could be reproduced. After a ^{68}Ga–^{68}Ge transmission scan (30 min) and the first PET scan, the monkey was moved to an operating table and MCA occlusion was performed under an operating microscope. A craniotomy was drilled superolateral to the optic nerve. After the dura was opened, the MCA occlusion was performed with 2 microvascular clips, 1 on the proximal part of the main MCA trunk and the other on the distal-to-orbitofrontal branch. On completion of the occlusion procedure, the monkey was again fixed in the stereotactic apparatus in the PET camera, and after a ^{68}Ga–^{68}Ge transmission scan (30 min), further PET scanning was performed. In the case of transient MCA occlusion, the 2 microvascular clips were removed 3 h after placement, without removing the animal from the stereotactic apparatus in the PET camera. During the experiments, the animal's body temperature was maintained within normal limits with heating blankets.

PET Studies

Four consecutive PET studies were performed on each monkey. Serial PET scanning was performed with the SHR7700 system, which has a transaxial resolution of 2.6 mm full width at half maximum (*14*). The first scan was obtained before MCA occlusion (mean, −92 ± 10 min). The second scan was obtained 124 ± 6 min after the start of occlusion. For the transient model, the third and fourth scans were obtained 200 ± 11 min and 362 ± 3 min after occlusion. For the permanent model, the third and fourth scans were obtained 240 ± 9 min and 363 ± 5 min after occlusion. CBF, $CMRO_2$, OEF, and local cerebral blood volume were assessed using the steady-state ^{15}O inhalation method (*11,12,15–17*), with successive inhalation of trace amounts of $C^{15}O_2$ (0.8 GBq/min), $^{15}O_2$ (2 GBq/min), and $C^{15}O$ (4 GBq/min). Each type of ^{15}O gas was administered through a ventilator (15 strokes/min, 70 mL/stroke). The $C^{15}O_2$ and $^{15}O_2$ scans were started after saturation of radioactivity in the gantry of the PET camera; the $C^{15}O$ scan was started 2 min after 20 s of $C^{15}O$ gas inhalation. Each scan consisted of 5 intervals of 1 min, for a total of 5 min. During each scan, 2 arterial blood samples were taken (1 at the beginning of the acquisition and 1 at the end) for whole-blood and plasma radioactivity measurements. The mean values of radioactivity for whole blood and plasma were used for parametric image generation (*17*).

TABLE 2
Physiologic Parameters in Model of Permanent Occlusion of Middle Cerebral Artery

Parameter	Before ischemia	Time after ischemia		
		2 h	4 h	6 h
MABP (mm Hg)	97 ± 6	108 ± 12	96 ± 16	98 ± 8
HR (bpm)	156 ± 23	171 ± 6	168 ± 7	172 ± 19
RT (°C)	37.0 ± 0.3	36.8 ± 0.4	37.3 ± 0.7	37.0 ± 0.4
pH	7.485 ± 0.032	7.470 ± 0.056	7.477 ± 0.051	7.467 ± 0.036
pCO_2 (mm Hg)	35.5 ± 4.1	36.2 ± 7.6	34.8 ± 5.7	34.9 ± 4.6
pO_2 (mm Hg)	172.9 ± 21.0	177.5 ± 28.0	171.7 ± 34.1	166.9 ± 28.1
Glucose (g/L)	82.8 ± 6.9	82.8 ± 10.1	82.6 ± 9.2	86.1 ± 13.0

MABP = mean arterial blood pressure; HR = heart rate; RT = rectal temperature; pCO_2 = partial pressure of carbon dioxide; pO_2 = partial pressure of oxygen.
Data are mean ± SD.

The calculated $CMRO_2$ and OEF values were obtained after cerebral blood volume correction.

Regions of Interest

Regions of interest (ROIs) were chosen by comparing the CBF in the ipsilateral hemisphere against that in the contralateral hemisphere 2 h after MCA occlusion. Areas of 0%–10%, 11%–20%, 21%–30%, 31%–40%, 41%–50%, 51%–60%, and >60% CBF reduction were defined as ROIs, and the changes in all parameters were calculated at all time points for each ROI. These ROIs were transposed by an image analysis system (Alice; Hayden Image Processing Group, Boulder, CO) to the PET images for all other parameters in the manner stated above at all time points studied. In this study, the results cover a 4-mm region from the anterior commissure, because there the changes were constant. The validity of the data was checked by calculation of preischemic values (theoretic value is 1).

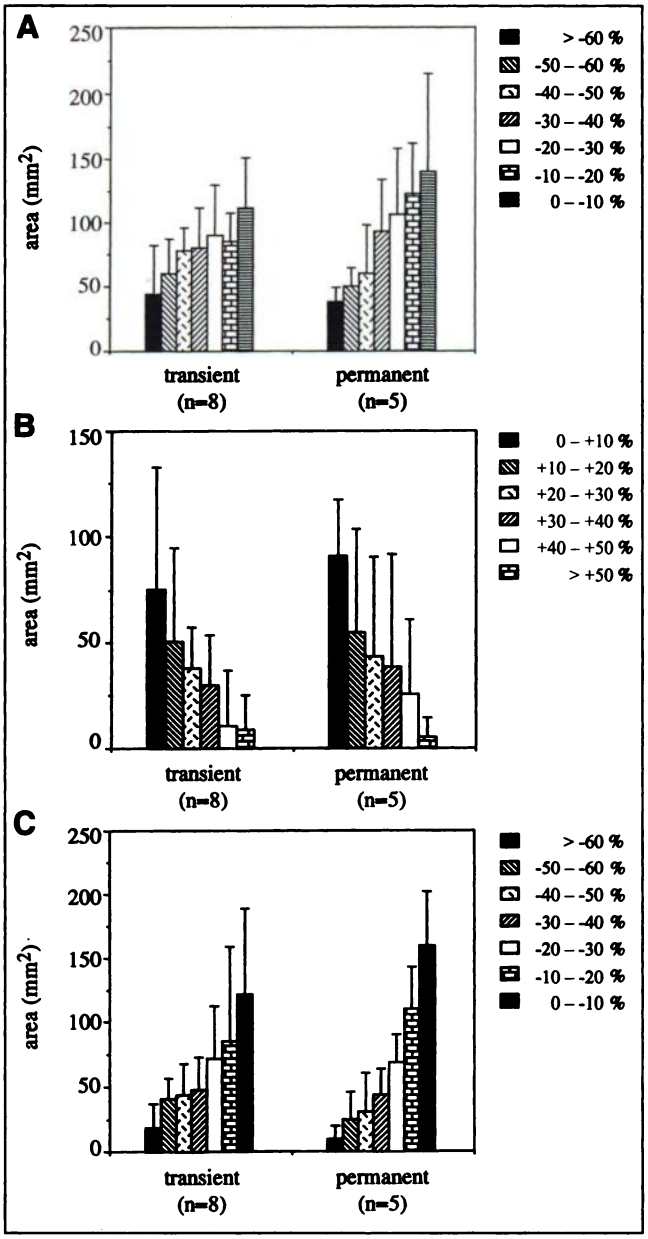

FIGURE 1. Comparison of ischemic conditions between transient and permanent models. Two hours after ischemia, areas of 0%–10%, 11%–20%, 21%–30%, 31%–40%, 41%–50%, 51%–60%, and >60% CBF decrease (A), OEF increase (B), and $CMRO_2$ decrease (C) in ipsilateral hemisphere relative to contralateral hemisphere were determined.

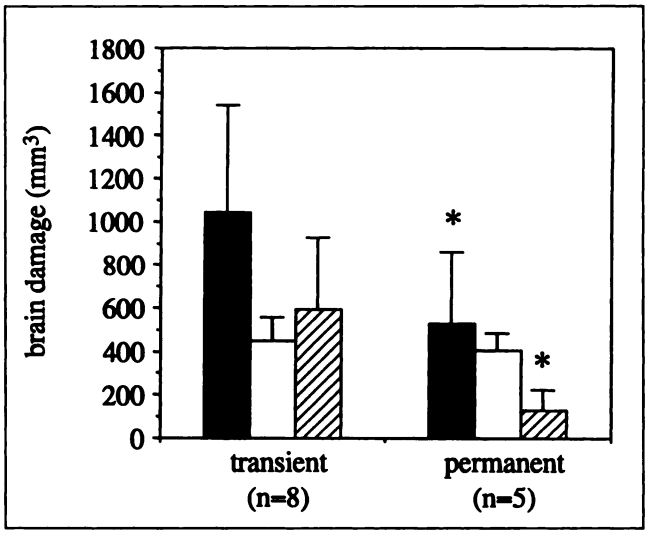

FIGURE 2. Comparison of brain damage 8 h after MCA occlusion between transient and permanent models. Black bars represent total brain damage; white bars, brain damage in basal ganglia; and shaded bars, cortical damage. *Significantly ($P < 0.05$) different from value for transient MCA occlusion group.

Neuropathology

Eight hours after the completion of MCA occlusion, the monkeys were deeply anesthetized with sodium pentobarbital. The brain was fixed by transcardial perfusion with a 10% formalin neutral buffer solution, pH 7.4, after saline perfusion at 100 mm Hg. The brain was then removed, and 12 coronal sections at 2-mm intervals were cut using a brain matrix (MBM-2000C; Bioresearch Center, Nagoya, Japan). Each section was embedded in paraffin, and 10-μm-thick sections were cut and stained with hematoxylin-eosin. The extent of brain edema was examined according to the method of Swanson et al. (*18*). The neuronal damage in each section was defined (*19*), and after correction for brain edema (*18*), the area of neuronal damage was measured using a computerized image analysis system. The volumes of neuronal damage were calculated from the areas of damage in the coronal sections and their anteroposterior coordinates.

MRI

Each monkey underwent MRI with a 0.5-T MRT-50A/II scanner (Toshiba, Tokyo, Japan) no less than 3 d before the MCA occlusion experiment. Under pentobarbital anesthesia, the monkeys were fixed in a plastic stereotactic apparatus, as for the PET studies, and T1-weighted images (transaxial resolution, 0.586 mm; slice–slice interval, 3 mm) were obtained (*20,21*).

Data Analysis

Changes in CBF, OEF, and $CMRO_2$ were calculated by comparing the values in the right and left (ipsilateral and contralateral) hemispheres of individual ROIs and are reported as right-to-left ratios. Data are presented as mean ± SD. Physiologic and biochemical data were evaluated by ANOVA and the Dunnett multiple comparisons test. The unpaired *t* test was used when only 2 groups were involved. $P < 0.05$ was considered significant.

RESULTS

Physiologic variables during the prolonged experiments remained within the normal range (Tables 1 and 2). Figure 1 shows the areas of CBF, OEF, and $CMRO_2$ changes 2 h after MCA occlusion in both the transient and the permanent models. The degree of ischemia between these models was compared by calculating the areas of serial phased CBF decrease, OEF increase, and $CMRO_2$ decrease. No significant difference was found.

Both transient and permanent MCA occlusion caused necrotic brain damage 8 h after ischemia. The damage occurred in the cortex and the basal ganglia (mainly in the putamen and caudate nucleus). Hemorrhage in the vicinity of the lesion was not found. However, the volume of the right hemisphere was increased by edema formation. The ratio of the right to the left hemisphere in the transient model was 1.17 ± 0.05, and that in the permanent model was 1.09 ± 0.03. The area of brain damage after correction for swelling was 1040.2 ± 496.7 mm^3 (cortex, 591.9 ± 330.8 mm^3; basal ganglia, 448.3 ± 106.9 mm^3) in the transient model and 530.9 ± 326.8 mm^3 (cortex, 128.3 ± 96.9 mm^3; basal ganglia, 402.6 ± 82.3 mm^3) in the permanent model (Fig. 2). Total and cortical brain damage were both significantly less after permanent MCA occlusion than after transient MCA occlusion.

Figure 3 shows the CBF, OEF, and $CMRO_2$ changes in the transient and permanent models. MCA occlusion decreased CBF and $CMRO_2$ and increased OEF. In the permanent model, these changes were constant throughout the experiment. In the transient model, the reperfusion caused postischemic hyperperfusion ($P < 0.05$) immediately after reperfusion and postischemic hypoperfusion ($P < 0.05$) 3 h after reperfusion. The postischemic hypoperfusion was observed within the area of more than a 40% CBF decrease. OEF was increased by ischemia. The CBF threshold for the OEF increase was a 21–50% reduction. $CMRO_2$ was also decreased significantly ($P < 0.05$) by MCA occlusion. The CBF threshold for the $CMRO_2$ decrease was more than a 50% reduction. In the transient model, the $CMRO_2$ decrease was partially recovered by reperfusion, but a further significant decrease was observed 3 h after reperfusion.

Figures 4 and 5 show typical images of CBF, OEF, and $CMRO_2$ changes in the transient and permanent models, their corresponding MRI images, and the results of hematoxy-

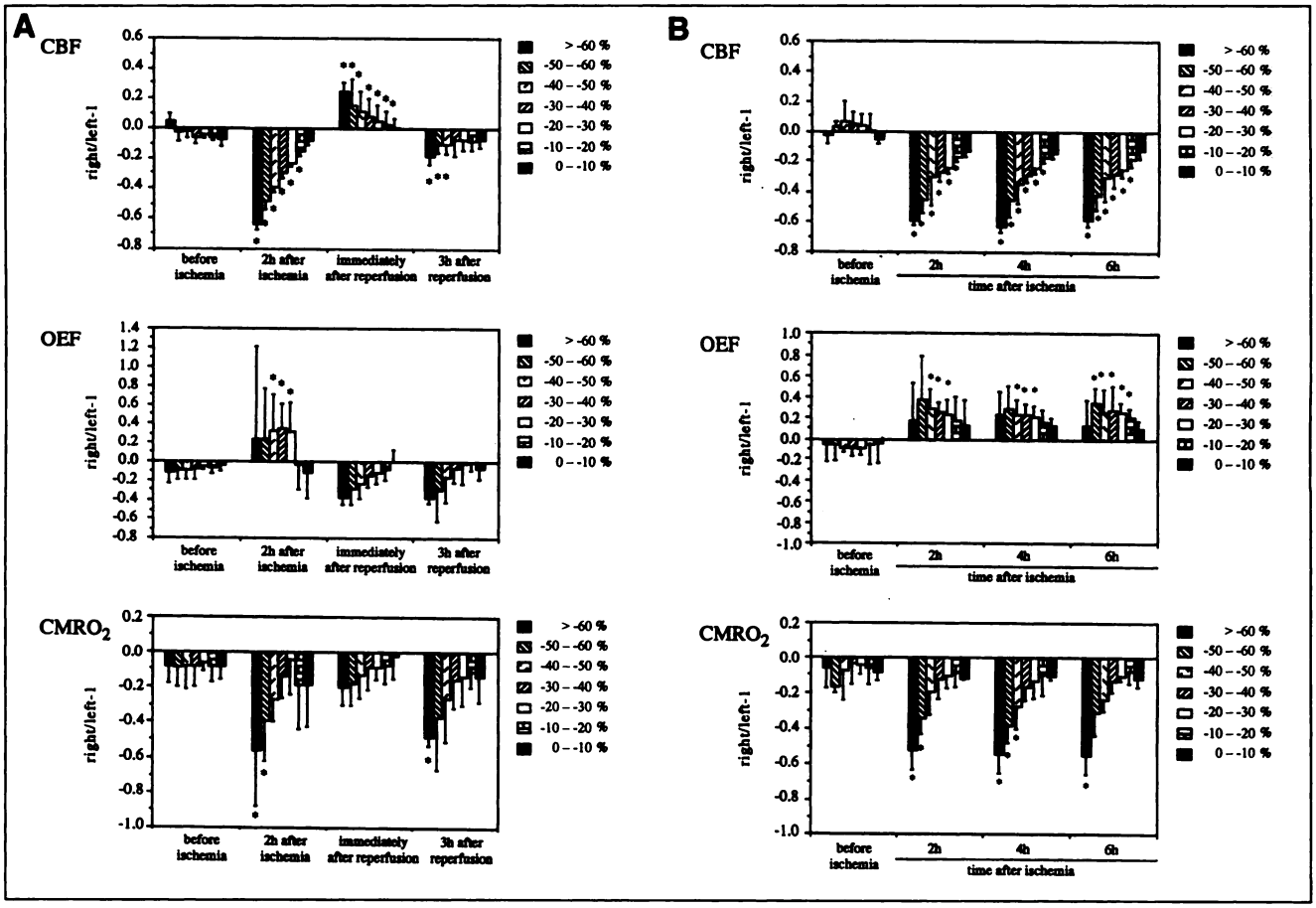

FIGURE 3. Time courses of CBF, OEF, and $CMRO_2$ changes in transient (A) and permanent (B) MCA occlusion models. ROIs were chosen on the basis of extent (0%–10%, 11%–20%, 21%–30%, 31%–40%, 41%–50%, 51%–60%, and >60%) of decrease of CBF in ipsilateral hemisphere relative to that in contralateral hemisphere 2 h after MCA occlusion. *Significantly ($P < 0.05$) different from value before MCA occlusion.

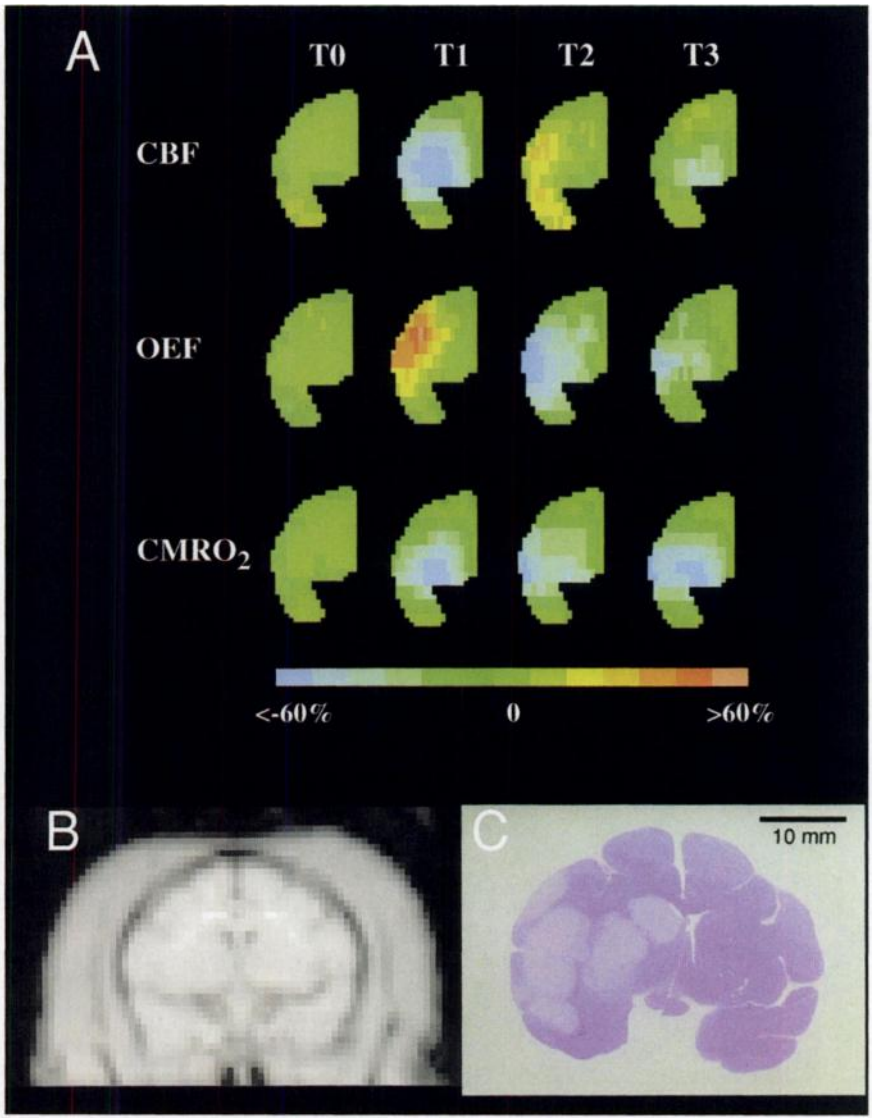

FIGURE 4. Sequential PET images (A) of transient ischemia in cynomolgus monkey 7 showing CBF, OEF, and $CMRO_2$; corresponding MRI image (B); and hematoxylin-eosin stained section (C) 8 h after MCA occlusion. PET image uses gradient scale that shows 0%–10%, 11%–20%, 21%–30%, 31%–40%, 41%–50%, 51%–60%, and >60% decrease and increase in ipsilateral hemisphere relative to contralateral hemisphere. T0, T1, T2, and T3 indicate time points before MCA occlusion, 2 h after MCA occlusion, immediately after reperfusion, and 3 h after reperfusion, respectively.

lin-eosin staining 8 h after ischemia. Each PET image shows the gradient changes after calculation of the right-to-left ratio from the PET image. The gradient range was from a $<-60\%$ change to a $>60\%$ change, with each color showing a 10% change. During ischemia, the areas of CBF and $CMRO_2$ decrease were similar, situated deep in the MCA territory, but the OEF increase occurred in the cortex (Figs. 4A [T1] and 5A [P1, P2, and P3]). After reperfusion, postischemic hyperperfusion was observed in the cortex, as were the OEF and $CMRO_2$ decreases.

Six hours after MCA occlusion, the areas of serial phased $CMRO_2$ decrease in the transient and permanent models were compared (Fig. 6A). The area of more than a 40% decrease in the ipsilateral hemisphere relative to the contralateral hemisphere was larger for the transient model. The total area of more than a 40% decrease was 163.6 ± 82.5 mm^2 in the transient model and 70.3 ± 44.3 mm^2 in the permanent model. Brain damage 8 h after ischemia correlated well with the areas of more than a 40% $CMRO_2$ decrease ($r = 0.747$; $P = 0.0034$; Fig. 6B).

DISCUSSION

We investigated hemodynamic changes and oxygen metabolism after temporary (3 h) and permanent occlusion of MCA in anesthetized cynomolgus monkeys using PET. Our purpose was to determine whether reperfusion injury can be detected with PET and to clarify the extent to which reperfusion contributes to brain damage. We compared functional changes and neuropathologic changes in the brain during the acute phase of ischemia and reperfusion.

MCA occlusion decreased CBF and $CMRO_2$ and increased OEF. These observations have commonly been observed in PET studies of focal cerebral ischemia (*10–12,15,22–25*). Because the area of neuronal damage depends on the extent of blood flow reduction and the duration of ischemia (*26,27*), we chose areas of serial phased CBF decrease as ROIs and compared the CBF, OEF, and $CMRO_2$ in each ROI between the 2 models.

We compared the degree of ischemia by comparing the area of serial phased CBF, OEF, and $CMRO_2$ changes 2 h

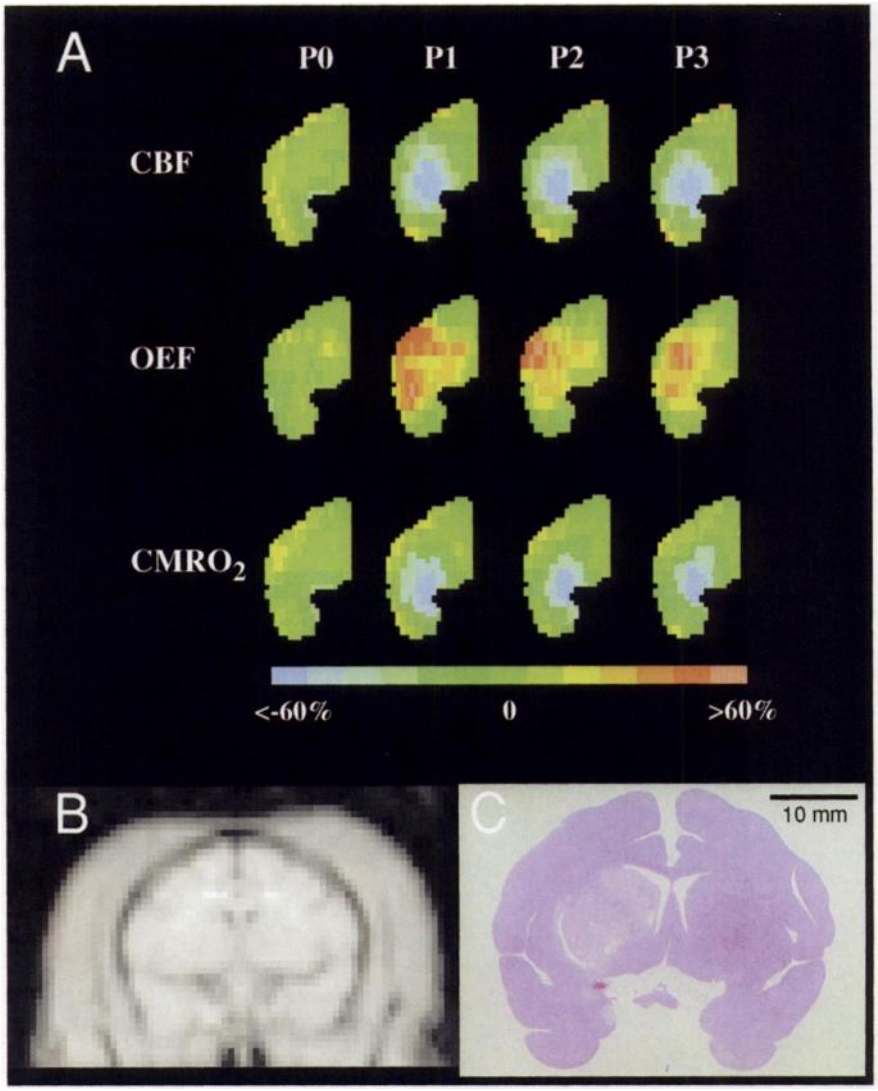

FIGURE 5. Sequential PET images (A) of permanent ischemia in cynomolgus monkey 2 showing CBF, OEF, and $CMRO_2$; corresponding MRI image (B); and hematoxylin-eosin stained section (C) 8 h after MCA occlusion. PET image uses gradient scale that shows 0%–10%, 11%–20%, 21%–30%, 31%–40%, 41%–50%, 51%–60%, and >60% decrease and increase in ipsilateral relative to contralateral hemisphere. P0, P1, P2, and P3 indicate time points before and 2, 4, and 6 h after MCA occlusion, respectively.

after MCA occlusion (Fig. 1) and found no significant differences between the transient and the permanent models. However, brain damage in the transient model was approximately twice that in the permanent model and therefore may have been induced by reperfusion. Cortical damage was greatest in the transient model, indicating that reperfusion may have contributed strongly to the cortical damage in this study.

We analyzed PET images to determine what happened in the cortical areas that showed a phenomenon resembling reperfusion injury. During ischemia, the transient model showed a decrease in CBF and $CMRO_2$ and an increase in OEF. CBF and $CMRO_2$ were decreased in the deep MCA territory but not in the cortex. OEF increased in an area of mild ischemia (21%–50% decrease in CBF) that was composed mainly of cortex. The permanent model showed an increased OEF in the cortex as well, but this area was not injured. Young et al. (*15*) also showed that the OEF increase during ischemia was not an indicator of inescapable consolidated infarction. Immediately after reperfusion, postischemic hyperperfusion was observed in the cortical area in which necrotic brain damage was observed. In these hyperperfused areas, a region of OEF and $CMRO_2$ decrease was shown (Fig. 4). The $CMRO_2$ decrease in the deep MCA area was partially recovered immediately after reperfusion; however, 3 h after reperfusion, $CMRO_2$ again decreased and spread to the cortex, in which the OEF and $CMRO_2$ decreased immediately after reperfusion.

We considered a $CMRO_2$ decrease 3 h after reperfusion to reflect neuronal damage, because Touzani et al. (*12,28*) reported a relationship between the infarct volumes and the area of more than a 40% $CMRO_2$ decrease in studies of both permanent and temporary MCA occlusion in baboon models at chronic stages. We also confirmed that the area of more than a 40% $CMRO_2$ decrease 6 h after ischemia in the transient model was significantly larger than that in the permanent model. These areas correlated well with brain damage 8 h after ischemia (Fig. 6). Our observations support the findings of Touzani et al. and suggest that a threshold of more than 40% $CMRO_2$ decrease in the ipsilateral hemisphere relative to the contralateral hemisphere may also be the best indicator of acute brain damage.

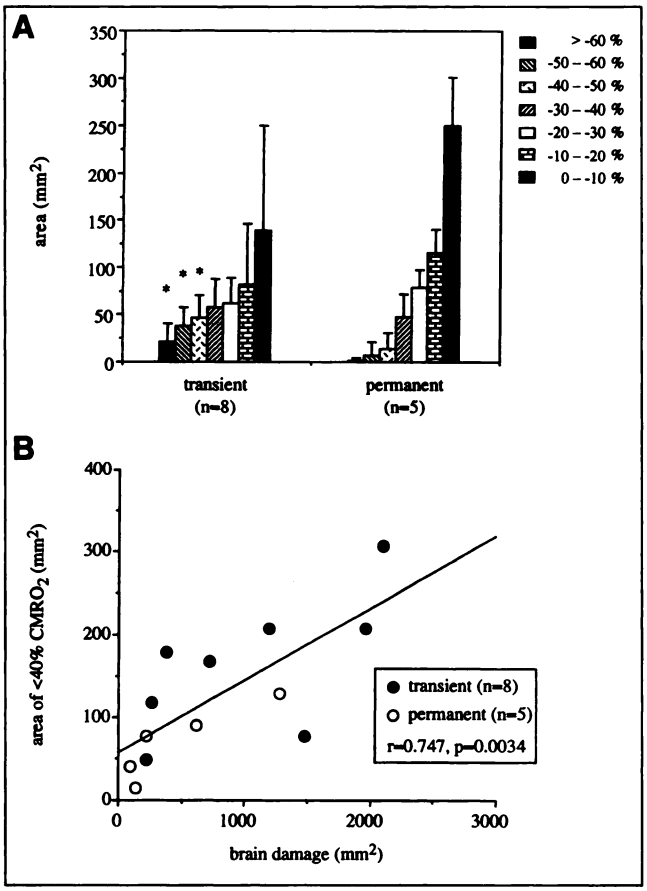

FIGURE 6. (A) Comparison of area of reduction of $CMRO_2$ 6 h after MCA occlusion between transient and permanent ischemia models. Areas of 0%–10%, 11%–20%, 21%–30%, 31%–40%, 41%–50%, 51%–60%, and >60% $CMRO_2$ decrease in ipsilateral relative to contralateral hemisphere were calculated. *Significantly ($P < 0.05$) different from value for permanent ischemia. (B) Correlation between brain damage 8 h after ischemia (in square millimeters) and areas of more than 40% $CMRO_2$ decrease 6 h after MCA occlusion (in square millimeters).

The OEF increase during ischemia reflects an inadequate supply of oxygen for underlying metabolic needs. Hyperperfusion after reperfusion provides an excess of oxygen that may be adequate for reactive oxygen radical production, which may accelerate brain damage. Therefore, the OEF and $CMRO_2$ decrease in the cortical area immediately after reperfusion may indicate reperfusion injury.

In our transient model, postischemic hypoperfusion occurred 3 h after reperfusion. This phenomenon was observed in the area with more than a 50% CBF decrease during ischemia—a region corresponding to the deep MCA territory and part of the cortex. The observations of hypoperfusion are consistent with those reported by Heiss et al. (*22*). According to the results of del Zoppo et al. (*29*) and Mori et al. (*30*), a time point 3 h after the completion of reperfusion after 3 h of ischemia was adequate to investigate the no-reflow phenomenon. They examined the patency of capillaries and the effect of capillary-obstructing polymorphonuclear leukocytes (*29,30*). The hypoperfusion observed in our study may be caused by the no-reflow phenomenon. This phenomenon may contribute to brain damage, especially in the late phase of ischemia–reperfusion.

CONCLUSION

We compared transient and permanent models of MCA occlusion in cynomolgus monkeys by PET. Overall, brain damage was significantly greater in the transient model than in the permanent model. Cortical damage in the transient model was distinct from that in the permanent model. These results suggest that reperfusion may strongly contribute to cortical damage. The results of PET studies showed that a peculiar OEF and $CMRO_2$ decrease in the cortical area occurred immediately after reperfusion. These changes may indicate reperfusion injury. Reperfusion injury may be caused not only by an excess of oxygen but also by the change in intracranial pressure, such as from edema formation after damage of endothelial function or the blood–brain barrier. However, in this study, particular damage occurred in the area of excessive hyperperfusion. Although this PET study had several limitations, PET images combined with histologic analysis in the acute phase of ischemia or ischemia–reperfusion showed peculiar changes in oxygen metabolism induced by reperfusion in the damaged area.

ACKNOWLEDGMENT

This study was supported in part by the Strategic Promotion System for Brain Science of the Science and Technology Agency of the Japanese government.

REFERENCES

1. Chan PH. Oxygen radicals in focal cerebral ischemia. *Brain Pathol.* 1994;4: 59–65.
2. Chan PH. Role of oxidants in ischemic brain damage. *Stroke.* 1994;27:1124–1129.
3. Yang G-Y, Betz AL. Reperfusion-induced injury to the blood-brain barrier after middle cerebral artery occlusion in rats. *Stroke.* 1994;25:1658–1665.
4. Abe K, Yuki S, Kogure K. Strong attenuation of ischemic and postischemic brain edema in rats by a novel free radical scavenger. *Stroke.* 1988;19:480–485.
5. Clemens JA, Saunders RD, Ho PP, Phebus RA, Panetta JA. The antioxidant LY231617 reduces global ischemic neuronal injury in rats. *Stroke.* 1993;24:716–723.
6. Kil HY, Zhang J, Piantadosi CA. Brain temperature alters hydroxyl radical production during cerebral ischemia/reperfusion in rats. *J Cereb Blood Flow Metab.* 1996;16:100–106.
7. Morimoto T, Globus MYT, Busto R, Martinez E, Ginsberg MD. Simultaneous measurement of salicylate hydroxylation and glutamate release in the penumbral cortex following transient middle cerebral artery occlusion. *J Cereb Blood Flow Metab.* 1996;16:92–99.
8. Patt A, Horesh IR, Berger EM, Harken AH, Repine JE. Iron depletion or chelation reduces ischemia/reperfusion-induced edema in gerbil brain. *J Pediatr Surg.* 1990;25:224–228.
9. National Institute of Neurological Disorders and Stroke rt-PA Stroke Study Group. Tissue plasminogen activator for acute ischemic stroke. *N Engl J Med.* 1995;333: 1581–1587.
10. Tenjin H, Ueda S, Mizukawa N, et al. Positron emission tomographic measurement of acute hemodynamic changes in primate middle cerebral artery occlusion. *Neurol Med Chir (Tokyo).* 1992;32:805–810.
11. Pappata S, Fiorelli M, Rommel T, et al. PET study of changes in local brain hemodynamics and oxygen metabolism after unilateral middle cerebral artery occlusion in baboons. *J Cereb Blood Flow Metab.* 1993;13:416–426.
12. Touzani O, Young AR, Derlon J-M, et al. Sequential studies of severely hypometabolic tissue volumes after permanent middle cerebral artery occlusion: a

positron emission tomographic investigation in anesthetized baboons. *Stroke.* 1995;26:2112–2119.
13. Hudgins WR, Garcia JH. Transorbital approach to the middle cerebral artery of squirrel monkey: a technique for experimental cerebral infarction applicable to ultrastructural studies. *Stroke.* 1970;1:107–111.
14. Watanabe M, Okada H, Shimizu K, et al. A high resolution animal PET scanner using compact PS-PMT detectors. *IEEE Trans Nucl Sci.* 1997;44:1277–1282.
15. Young AR, Sette G, Touzani O, et al. Relationships between high oxygen extraction fraction in the acute stage and final infarction in reversible middle cerebral artery occlusion: an investigation in anesthetized baboons with positron emission tomography. *J Cereb Blood Flow Metab.* 1996;16:1176–1188.
16. Frackowiak RSJ, Lenzi GL, Jones T, Hearther JD. Quantitative measurement of regional cerebral blood flow and oxygen metabolism in man using ^{15}O and positron emission tomography: theory, procedure and normal values. *J Comput Assist Tomogr.* 1980;4:727–736.
17. Sette G, Baron JC, Mazoyer B, Levasseur M, Pappata S, Crouzel C. Local brain haemodynamics and oxygen metabolism in cerebrovascular disease: positron emission tomography. *Brain.* 1989;112:931–951.
18. Swanson RA, Morton MT, Tsao-Wu G, Savalos RA, Davidson C, Sharp FR. A semiautomated method for measuring brain infarct volume. *J Cereb Blood Flow Metab.* 1990;10:290–293.
19. Osborne KA, Shigeno T, Balarsky A-M, et al. Quantitative assessment of early brain damage in a rat model of focal cerebral ischemia. *J Neurosurg Psychiatry.* 1987;50:402–410.
20. Takechi H, Onoe H, Imamura K, et al. Brain activation study by use of positron emission tomography in unanesthetized monkeys. *Neurosci Lett.* 1994;182:279–282.
21. Tsukada H, Kakiuchi T, Ando I, Ouchi Y. Functional activation of cerebral blood flow abolished by scopolamine is reversed by cognitive enhancers associated with cholinesterase inhibition: a positron emission tomography study in unanesthetized monkeys. *J Pharmacol Exp Ther.* 1997;281:1408–1414.
22. Heiss W-D, Graf R, Löttgen J, et al. Repeat positron emission tomographic studies in transient middle cerebral artery occlusion in cats: residual perfusion and efficacy of postischemic reperfusion. *J Cereb Blood Flow Metab.* 1997;17:388–400.
23. Heiss W-D, Graf R, Wienhard K, et al. Dynamic penumbra demonstrated by sequential multitracer PET after middle cerebral artery occlusion in cats. *J Cereb Blood Flow Metab.* 1994;14:892–902.
24. Baron JC. Pathophysiology of acute cerebral ischemia: PET studies in humans. *Cerebrovasc Dis.* 1991;1(suppl 1):22–31.
25. Marchal G, Serrati C, Rioux P, et al. PET imaging of cerebral perfusion and oxygen consumption in acute ischemic stroke: relation to outcome. *Lancet.* 1993;341:2–4.
26. Crowell RM, Marcoux FW, Deirolami U. Variability and reversibility of focal cerebral ischemia in unanesthetized monkeys. *Neurology.* 1981;31:1295–1302.
27. Jones TH, Morawetz RB, Crowell RM, et al. Thresholds of focal cerebral ischemia in awake monkeys. *J Neurosurg.* 1981;54:773–782.
28. Touzani O, Young AR, Derlon J-M, Baron J-C, MacKenzie ET. Progressive impairment of brain oxidative metabolism reversed by reperfusion following middle cerebral artery occlusion in anaesthetized baboons. *Brain Res.* 1997;767:17–25.
29. del Zoppo GJ, Schmid-Schonbein GW, Mori E, Copeland BR, Chang C-M. Polymorphonuclear leukocytes occlude capillaries following middle cerebral artery occlusion and reperfusion in baboons. *Stroke.* 1991;22:1276–1283.
30. Mori E, del Zoppo GJ, Chambers JD, Copeland BR, Arfors K-E. Inhibition of polymorphonuclear leukocytes adherence suppresses no-reflow after focal cerebral ischemia in baboons. *Stroke.* 1992;23:712–718.